



Article

MYRF: A New Regulator of Cardiac and Early Gonadal Development—Insights from Single Cell RNA Sequencing Analysis

Verónica Calonga-Solís ^{1,2}, Helena Fabbri-Scaliet ^{1,3}, Fabian Ott ², Mostafa Al-Sharkawi ^{1,4}, Axel Künstner ², Lutz Wunsch ⁵, Olaf Hiort ¹, Hauke Busch ² and Ralf Werner ^{1,6,*}

- ¹ Division of Paediatric Endocrinology and Diabetes, Department of Paediatric and Adolescent Medicine, University of Lübeck, 23562 Lübeck, Germany
- ² Medical Systems Biology Division, Lübeck Institute of Experimental Dermatology, University of Lübeck, 23562 Lübeck, Germany
- ³ Center for Molecular Biology and Genetic Engineering—CBMEG, State University of Campinas, Campinas 13083-875, Brazil
- ⁴ Biochemical Genetics Department, Human Genetics and Genome Research Institute, National Research Centre, Dokki, Cairo 12622, Egypt
- ⁵ Department of Pediatric Surgery, University of Lübeck, 23562 Lübeck, Germany
- ⁶ Institute of Molecular Medicine, University of Lübeck, 23562 Lübeck, Germany
- * Correspondence: ralf.werner@uni-luebeck.de



Citation: Calonga-Solís, V.; Fabbri-Scaliet, H.; Ott, F.; Al-Sharkawi, M.; Künstner, A.; Wunsch, L.; Hiort, O.; Busch, H.; Werner, R. MYRF: A New Regulator of Cardiac and Early Gonadal Development—Insights from Single Cell RNA Sequencing Analysis. *J. Clin. Med.* **2022**, *11*, 4858. <https://doi.org/10.3390/jcm11164858>

Academic Editor: K. Katharina Rall

Received: 30 June 2022

Accepted: 17 August 2022

Published: 18 August 2022

Publisher's Note: MDPI stays neutral with regard to jurisdictional claims in published maps and institutional affiliations.



Copyright: © 2022 by the authors. Licensee MDPI, Basel, Switzerland. This article is an open access article distributed under the terms and conditions of the Creative Commons Attribution (CC BY) license (<https://creativecommons.org/licenses/by/4.0/>).

Abstract: De novo variants in the myelin regulatory factor (MYRF), a transcription factor involved in the differentiation of oligodendrocytes, have been linked recently to the cardiac and urogenital syndrome, while familiar variants are associated with nanophthalmos. Here, we report for the first time on a patient with a de novo stop-gain variant in *MYRF* (p.Q838*) associated with Scimitar syndrome, 46,XY partial gonadal dysgenesis (GD) and severe hyperopia. Since variants in *MYRF* have been described in both 46,XX and 46,XY GD, we assumed a role of *MYRF* in the early development of the bipotential gonad. We used publicly available single cell sequencing data of human testis and ovary from different developmental stages and analysed them for *MYRF* expression. We identified *MYRF* expression in the subset of coelomic epithelial cells at stages of gonadal ridge development in 46,XX and 46,XY individuals. Differential gene expression analysis revealed significantly upregulated genes. Within these, we identified *CITED2* as a gene containing a MYRF binding site. It has been shown that *Cited2*^{-/-} mice have gonadal defects in both testis and ovary differentiation, as well as defects in heart development and establishment of the left–right axis. This makes *MYRF* a potential candidate as an early regulator of gonadal and heart development via upregulation of the transcriptional cofactor *CITED2*.

Keywords: *MYRF*; *CITED2*; scimitar syndrome; disorders of sex development; gonadal development; cardiac and urogenital syndrome

1. Introduction

In 2009, the *MYRF* gene (*Myelin Regulatory Factor*, OMIM * 608329) was described as a critical transcriptional regulator required for the myelination of the central nervous system (CNS) [1]. Subsequently, studies characterized the function of *MYRF* as a membrane-associated transcription factor for oligodendrocyte differentiation, stimulating myelin gene expression in the CNS [2,3]. Currently, it is known that *MYRF* is also expressed in other tissues in addition to the CNS, especially during the early development of the diaphragm, heart, eyes, lungs and genitourinary tract, which is consistent with the fact that variants in this gene have been associated with congenital diaphragmatic hernia [4], congenital heart diseases [5], nanophthalmos and other ocular defects [6], and more recently, with a new cardiac and urogenital syndrome (CUGS), as well as with disorders/differences of sex

development (DSD) [7,8], a group of conditions in which development of chromosomal, gonadal or anatomic sex is atypical [9]. Sex determination in mammals is controlled by the interaction between many genes that drive a bistable embryonic gonadal development program. Testis and ovarian promoting pathways act as an antagonistic network system with a remarkable plasticity [10]. In the 46,XY gonad, the presence of SRY activates the *SOX9/FGF9* pathway, leading to testis development, Sertoli and Leydig cell formation and androgen production, resulting to internal and external virilization. In contrast, the absence of *SRY* in the 46,XX gonad will upregulate the *RSPO1/WNT4/b-catenin* pathway, repressing the *SOX9/FGF9* pathway to promote ovarian development, with granulosa and theca cells. In humans, a disruption in either pathway can result in gonadal dysgenesis, leading to a range of genital phenotypes between both sexes [11].

MYRF (previously known as *C11orf9* [12]), is located at 11q12.2 and expands around 35 kb of genomic DNA divided into 27 exons. It encodes for a 1151 amino acid protein, characterized by a proline-rich region containing a nuclear localization signal (NLS), a DNA-binding domain (DBD), an intramolecular chaperone auto-processed domain (ICA) (also known as Peptidase S74 domain), a transmembrane domain (TM) and two myelin gene regulatory factor C-terminal domains (MRF C1 and MRF C2) [3,12]. An intramolecular chaperone from the ICA domain helps *MYRF* to form a homo-trimer in the endoplasmic reticulum, which is essential for its biological process, where it carries out the auto-cleavage of *MYRF*, allowing it to function as a transcription factor in the nucleus [13].

Here, we report a novel, heterozygous de novo p.Q838* variant in *MYRF* in a patient with 46,XY partial gonadal dysgenesis (PGD), Scimitar syndrome and severe hyperopia, identified by whole genome analysis. Haploinsufficiency of *MYRF* has been identified as a cause of DSD in 46,XX and 46,XY individuals [7]; however, there is limited knowledge about the function of this gene and its influence on the molecular pathways in sex development. To elucidate the influence of *MYRF* expression on the developing gonads, we use previously published single cell RNA-seq data of human testes and ovaries. *CITED2* was found upregulated in *MYRF*-expressing cells and is possibly a downstream target of *MYRF*. We highlight the important role *MYRF* plays in early developmental stages of the undifferentiated gonad and how it can affect gonadal development of 46,XY and 46,XX individuals, as well as heart morphogenesis and establishment of the left–right axis.

2. Materials and Methods

2.1. Patient Description

The child was prenatally suspected of having a congenital heart defect with questionable situs inversus and anomalous pulmonary vein confluence. The birth was by caesarean section at gestational week 38 + 5. Genital status was not questioned at that time and a female sex was assigned. Scimitar syndrome was diagnosed with dextrocardia and an abnormal confluence of a right-sided pulmonary vein in the inferior vena cava. The right lung showed a rudimentary upper lobe bronchus that narrowed after 1 cm. Only one dorsal relatively small right upper lobe segment was present. The right lower lobe was pushed dorsally by the heart and was considerably compressed and partly atelectatic. Moreover, also belonging to the right lung, an overinflating lung segment was seen ventrobasally to the left of the heart. The well ventilated and fully expanded left lung was considerably larger than the right one. In addition, aside of the spleen, two small accessory spleens were seen. At the age of 6 months, the anomalous pulmonary veins became attached to the left atrium. A follow-up at the age of one year showed rarefaction in the right lower lobe of the lung.

At the age of 8 years, clitoris hypertrophy without signs of puberty became apparent and the child was seen by a paediatric endocrinologist. Apparently, both gonadotrophins and testosterone were elevated. She presented to our hospital endocrine unit at the age of 10 years for further assessment. At this time, she felt healthy and there were no imminent pulmonary or cardiovascular problems. She had no acne, no hirsutism, no breast development and was of normal height and weight. She had severe hyperopia with 9 dpt,

corrected with glasses. Her clitoris was 3.5 cm in length and the labia majora were rugated. LH was 5.7 IU/L (within the adult range), FSH 69.9 IU/L (above adult range), testosterone 0.51 µg/L (elevated for the female reference range, within the reference range of Tanner 2 pubertal development for boys). Additionally, 17-beta estradiol was below detection and inhibin B, at 9 pg/mL, was below the reference range for boys. On ultrasound, she had a small tubular structure behind the bladder, which was interpreted as a small rudimentary uterus. This was confirmed by MRI; gonads could not be visualised at that time. Urine steroid metabolome analysis revealed no signs of congenital adrenal hypoplasia. Subsequent karyotype analysis was 46,XY (ishYP11.3, SRY positive). Taken together, the findings were consistent with a 46,XY PGD. Puberty was stopped by a GnRH analogue. After gender assessment by a psychologist, puberty was induced at an appropriate age by estrogens/progestins. During follow-up, small gonads could be visualized by ultrasound or MRI in the inguinal canal and were examined every 12 months. Prophylactic gonadectomy was discussed repeatedly and a shared decision was made to delay the procedure until after her 18th birthday. Dextrocardia and hyperopia in conjunction with gonadal dysgenesis suggested a syndromic form of DSD. Array-CGH using a 180 k Microarray (Agilent) revealed an unsuspecting 46,XY karyotype without clinical relevant deletions or duplications (arr [hg19] 1–22)x2,(XY)x1). To elucidate the cause of this form of DSD, a whole genome sequencing analysis was initiated.

2.2. Whole Genome Sequencing (WGS)

WGS was performed to identify putative pathogenic variants, indels and structural variations. Sequencing libraries were constructed from 1.0 µg DNA per sample using the Truseq Nano DNA HT Sample Preparation Kit (Illumina, San Diego, CA, USA), following the recommendations of the manufacturer. Genomic DNA was randomly fragmented to a size of approximately 350 bp by Covaris cracker (Covaris, Woburn, MA, USA). DNA fragments were blunted, A-tailed and ligated with the full-length adapter for Illumina sequencing with further PCR amplification. Libraries were purified using AMPure XP (Beckman Coulter, Pasadena, CA, USA), analysed for size distribution on an Agilent 2100 Bioanalyser (Agilent Technologies, Santa Clara, CA, USA) and quantified by qPCR. Paired end sequencing of libraries was performed on Illumina HiSeq platforms (Illumina). Per sample, more than 90 GB of raw data were obtained, resulting in an average genomic read depth of 30×.

2.3. Bioinformatics

Sequencing reads were mapped to human reference genome version GRCh38 using the Burrows–Wheeler Aligner (BWA-MEM, v0.7.17) [14], and resulting mapping files were processed following GATK (Genome Analysis Toolkit) best practices for germline variant calling. Briefly, we screened for duplicated reads by applying *Mark Duplicates* from Picard tools (v.2.26.1, <http://broadinstitute.github.io/picard/>, accessed on 3 September 2021); split-reads and discordant paired-end alignments were extracted using *SAM tools* v0.1.18 [14] as implemented in (GATK, v.4.2.2.0) [15] with standard parameters. Single nucleotide variants (SNVs) and short insertions/deletions (InDels) were called using *Deep Variant* (v1.2.0). Detection of structural variants (SV) was performed using DELLY [16]. Variants were annotated using Ensembl Variant Effect Predictor—VEP (v103) (EMBL-EBI, Cambridge, UK). All chromosomal positions in the paper are according to GRCh38.

2.4. Single Cell RNA Analyses

We analysed publicly available single-cell RNA from testes and ovaries, which totalled 20 samples from testes of individuals at different stages, from embryo to adult men, and 4 samples of ovaries, from embryos and foetus [17–20] (for more detail, see the *Data Availability* section below and Supplementary Table S1). The scRNA sequences of these samples were obtained through the 10x Genomics sequencing platform. We pre-processed the raw sequences using fastp (v0.22.0) [21], which were later aligned and annotated to

the human reference cDNA GRCh38 with Kallisto (v0.46.1) and BUSStools (v0.39.3) [22]. This resulted in matrixes of UMI counts for each sample. The downstream filtering and analyses were performed with the R package Seurat v4.1.1 [23]. In brief, we retained genes expressed in at least three cells, and we kept cells if they had less than 25% reads mapping to the mitochondrial genome, if they had between 500 and 9000 genes, and if they had less than 40,000 mRNA molecules detected. We normalized the gene counts in each cell by the total cell expression, with the *Normalize Data* function, using log₁₀-transformation and a scale factor of 10,000. Integration of the samples was performed for testes and ovaries datasets separately, using *FindIntegration Anchors* and *Integrate Data* functions. Afterward, the cells were clustered by a shared nearest neighbour (SNN) modularity optimization and visualized in a two-dimensional space based on uniform manifold approximation and projection (UMAP). We classified the cell populations using the same marker genes as in the original publications [17–20] and other published literature [24,25].

To investigate which genes could have their expression affected by *MYRF*, we first subset the cell cluster of the coelomic epithelium (CE), the cell population that expressed this gene the highest. Later, we performed a differential expression analysis between the cells that express *MYRF* against those that do not express it, using the *FindMarkers* function with default parameters.

3. Results

We performed Trio-WGS (mother, father and affected child) and focused our analyses on protein-coding regions. SNVs and Indels were filtered for rare variants (frequency in 1 k project or gnomAD below 0.1%). A heterozygous de novo stop-gain variant in exon 20 of the myelin regulatory factor (*MYRF*) was detected (NM_001127392:c.2512C>T; p.Q838*) and confirmed by Sanger sequencing (Figure 1). According to the ACMG guidelines [26], this variant was considered pathogenic as it fulfils two criteria of the evidence of pathogenicity: PSV1 (classified as “null variant” since it is a nonsense variant) and PS1 (de novo variant confirmed by the absence in both parents). De novo variants in *MYRF* have been recently detected in patients with CUGS [27]. No further variants in genes associated with gonadal dysgenesis have been detected.

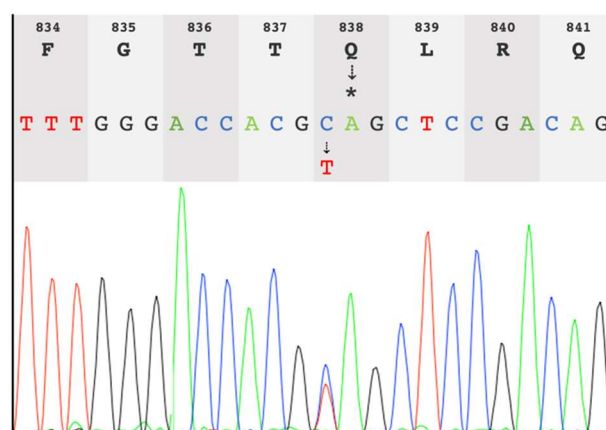


Figure 1. Sanger chromatogram showing the de novo heterozygous stop-gain variant in *MYRF* (c.2512C>T; p.Q838*) in the study patient.

Since variants in *MYRF* have been recently detected not only in 46,XY, but also 46,XX gonadal dysgenesis [7], we hypothesized that heterozygous inactivating variants may affect very early development of the bipotential gonad. Therefore, we reanalysed publicly available single cell RNA sequencing data (scRNA-seq) of different stages of human gonadal development to study the impact that *MYRF* could have in the early development of the gonads.

According to their stage or age, the testis samples were classified as embryonic, foetal, mini puberty, peri-puberty, pre-puberty and adults, and the ovary samples were classified

as embryonic or foetal (Supplementary Table S1). The reanalysis of these datasets yielded ~111,000 cells from testes and ~28,000 cells from the ovaries, which clustered in 20 and 19 cell populations, respectively (Figure 2), which were identified according to their distinctive gene expression (Supplementary Figures S1 and S2). In testes, clusters 1–7 were annotated as Leydig cells, clusters 8–10 as Sertoli cells. Cluster 11 was classified as mesonephric cells; however, it was also composed of cells with gene expression patterns of Leydig and Sertoli cells and was present mainly in the embryos and foetus. Cluster 12 was identified as coelomic epithelium cells and was also present mainly in embryos and foetus. Cluster 14–15 belonged to germ cells. The remaining clusters were classified as peritubular myoid, endothelial, macrophages and blood cells (Figure 2A). In ovaries, theca cells were found in cluster 1–6, granulosa cells in cluster 7–10, mesonephric cells in cluster 11 and coelomic epithelium cells in cluster 12. Germ cells were present in cluster 14–15 and the remaining cells were classified as smooth muscle, endothelial, macrophages and blood cells (Figure 2B).

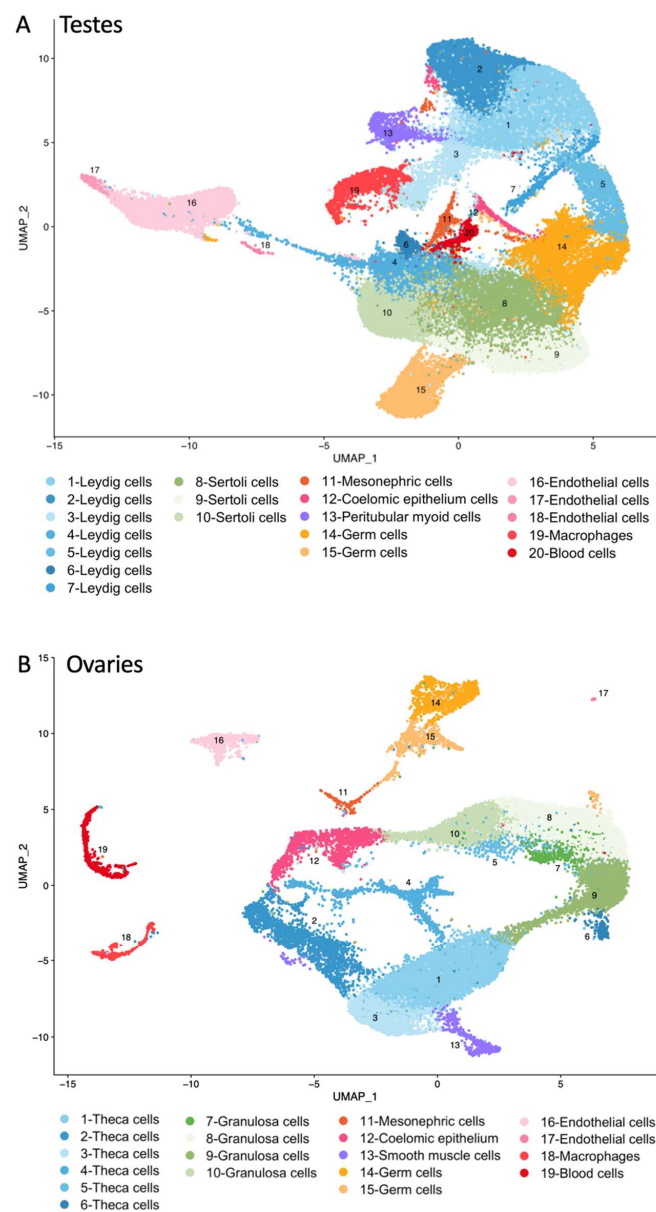


Figure 2. UMAP plots of cell clusters in human (A) testes from embryonic stage to adults; and (B) ovaries from embryonic and foetal stages identified by single cell RNA sequencing. UMAP: uniform manifold approximation and projection.

We observed that, in both testes and ovaries, *MYRF* is highly expressed in a subset of cells from the coelomic epithelium (CE) at embryonic and foetal stages (Figure 3), and that its expression is lowered after birth (Supplementary Figure S3). We aimed to search for genes that might be directly or indirectly regulated by this transcription factor. Therefore, we divided the cluster of CE cells into cells that express *MYRF* and those that do not, and investigated them for differentially expressed (DE) genes. We found 62 DE genes in the CE cells of testis and 13 genes in the CE of ovaries. Within this set of DE genes, approximal half of them (26 of the testis and 7 of the ovary genes) have *MYRF* binding sites according to the *GeneHancer* database [28] (Tables 1 and 2). One of these DE genes, the *CBP/p300-interacting transactivator with Glu/Asp-rich carboxy-terminal domain 2* (*CITED2*), is of particular interest, since it is a transcriptional cofactor that acts in the early stages of XX and XY gonadal development [29,30], and is involved in heart morphogenesis and establishment of the left–right axis [31].

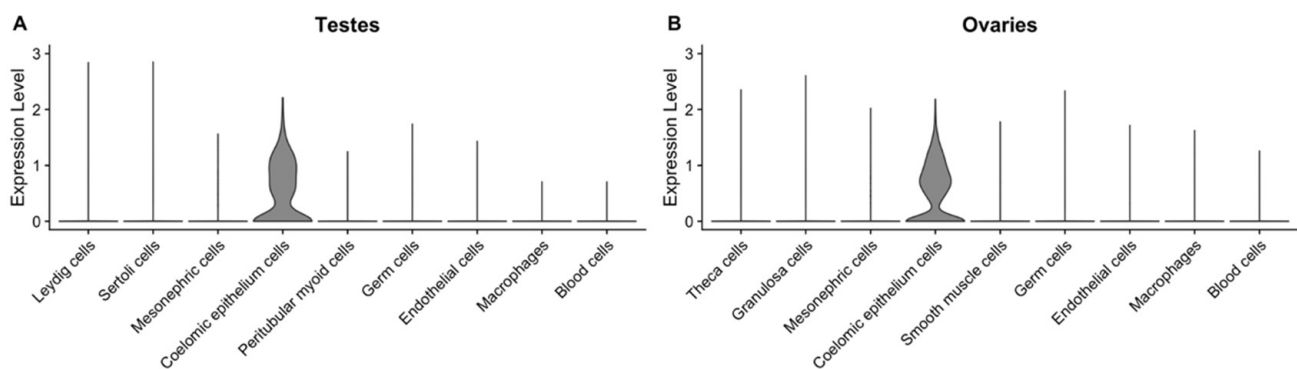


Figure 3. Expression levels of *MYRF* in testes (A) and ovaries (B) at embryonic and fetal stages, showing that it is highly expressed in coelomic epithelium cells.

Table 1. List of genes differentially expressed between the cells that express *MYRF* and those that do not, in the coelomic epithelium cluster of ovaries.

Female Samples									
DE Genes	Binding Site for <i>MYRF</i>	pct. <i>MYRF</i> (+)	pct. <i>MYRF</i> (–)	<i>p</i> -Value adj	DE Genes	Binding Site for <i>MYRF</i>	pct. <i>MYRF</i> (+)	pct. <i>MYRF</i> (–)	<i>p</i> -Value adj
<i>MYRF</i>	+	1	0	1.3608×10^{-261}	<i>ZFP36</i>	+	0.543	0.398	3.03465×10^{-5}
<i>NR4A1</i>	–	0.444	0.249	1.63171×10^{-10}	<i>IER2</i>	+	0.81	0.691	0.000188878
<i>SOCS3</i>	–	0.443	0.239	2.54304×10^{-10}	<i>CITED2</i>	+	0.672	0.474	0.000278465
<i>CRIP1</i>	–	0.509	0.322	5.59507×10^{-8}	<i>CALB2</i>	–	0.439	0.292	0.000329296
<i>FOSB</i>	+	0.568	0.383	1.88434×10^{-7}	<i>JUNB</i>	+	0.642	0.513	0.001629543
<i>EGR1</i>	+	0.631	0.464	1.82088×10^{-6}	<i>FOS</i>	–	0.775	0.693	0.006444703
<i>DUSP1</i>	+	0.644	0.459	3.9062×10^{-6}					

DE: differential expression analyses. *MYRF* (+): cells from coelomic epithelium that express at least one transcript of *MYRF*. *MYRF* (–): cells from coelomic epithelium that do not express any transcript of *MYRF*. Pct: percentage of cells where the gene is detected in *MYRF* (+) or (–) subsets.

Table 2. List of genes differentially expressed between the cells that express *MYRF* and those that do not, in the coelomic epithelium cluster of testes.

Male Samples									
DE Genes	Binding Site for <i>MYRF</i>	pct. <i>MYRF</i> (+)	pct. <i>MYRF</i> (–)	<i>p</i> -Value adj	DE Genes	Binding Site for <i>MYRF</i>	pct. <i>MYRF</i> (+)	pct. <i>MYRF</i> (–)	<i>p</i> -Value adj
<i>MYRF</i>	+	1	0	1.18×10^{-81}	<i>TNNI1</i>	–	0.764	0.45	0.001116
<i>H2AFX</i>	+	0.651	0.282	6.08×10^{-8}	<i>TMEM88</i>	–	0.455	0.187	0.001454
<i>C21orf58</i>	–	0.371	0.1	1.29×10^{-6}	<i>GGH</i>	–	0.48	0.201	0.001921
<i>HILPDA</i>	–	0.535	0.201	2.98×10^{-6}	<i>UBE2T</i>	–	0.455	0.211	0.001941
<i>DSG2</i>	+	0.549	0.211	3.24×10^{-6}	<i>MKI67</i>	–	0.404	0.163	0.002216
<i>DNMT1</i>	+	0.6	0.263	3.39×10^{-6}	<i>ZWINT</i>	–	0.484	0.22	0.002686

Table 2. Cont.

Male Samples									
DE Genes	Binding Site for MYRF	pct. MYRF (+)	pct. MYRF (−)	p-Value adj	DE Genes	Binding Site for MYRF	pct. MYRF (+)	pct. MYRF (−)	p-Value adj
ROBO1	−	0.484	0.172	8.73×10^{-6}	CDK1	−	0.418	0.172	0.002747
AURKB	+	0.458	0.163	2.32×10^{-5}	IDH2	+	0.698	0.407	0.003044
SGO1	−	0.371	0.11	3.15×10^{-5}	CDCA3	−	0.313	0.1	0.004612
GMNN	+	0.524	0.225	3.97×10^{-5}	PABPN1	+	0.76	0.488	0.004802
NOVA1	−	0.716	0.383	4.61×10^{-5}	MTRNR2L10	NA	0.825	0.526	0.006358
STX10	+	0.585	0.258	7.52×10^{-5}	PCNA	+	0.665	0.373	0.006529
UBE2S	+	0.625	0.335	9.06×10^{-5}	TYRO3	+	0.633	0.325	0.008898
CMSS1	−	0.622	0.297	0.000107	ECI1	+	0.596	0.306	0.009338
FEN1	−	0.447	0.172	0.000119	TK1	+	0.564	0.325	0.009615
SCARB2	+	0.629	0.306	0.000145	EIF3E	+	0.982	0.967	0.010135
RPSAP52	−	0.444	0.172	0.000187	LAPTM4B	−	0.895	0.67	0.011395
HNRNPAB	+	0.716	0.388	0.000202	CKS2	+	0.695	0.426	0.014009
YLPM1	−	0.407	0.148	0.000275	RABL6	−	0.651	0.368	0.01407
LIG1	+	0.349	0.11	0.000322	CENPF	−	0.524	0.282	0.015355
SMC1A	−	0.455	0.182	0.000419	AKR1B1	+	0.876	0.617	0.020538
SMC2	−	0.498	0.225	0.000429	BIRC5	+	0.545	0.311	0.021154
H2AFZ	−	0.942	0.823	0.00049	AURKA	+	0.255	0.077	0.021308
CENPM	−	0.44	0.177	0.000496	CBX5	−	0.931	0.732	0.022631
CENPV	−	0.647	0.368	0.000586	SMARCC1	+	0.771	0.464	0.022672
USP10	−	0.531	0.244	0.000751	UBE2C	+	0.542	0.297	0.023105
CDH3	−	0.531	0.249	0.000837	ZDHHC8P1	−	0.742	0.464	0.027005
ASFB1	+	0.302	0.086	0.000849	MAG	−	0.495	0.249	0.031231
HNRNPD	+	0.884	0.718	0.00087	SOX11	−	0.64	0.383	0.031795
ITGA3	−	0.596	0.292	0.000892	TPX2	+	0.375	0.153	0.035526
TMEM106C	−	0.68	0.411	0.000936	H2AFV	−	0.858	0.622	0.038892
FBXO5	−	0.367	0.129	0.000963					

DE: differential expression analyses. MYRF (+): cells from coelomic epithelium that express at least one transcript of MYRF. MYRF (−): cells from coelomic epithelium that do not express any transcript of MYRF. Pct: percentage of cells where the gene is detected in MYRF (+) or (−) subsets.

4. Discussion

The MYRF gene encodes a membrane-associated transcription factor, which has been recently identified as candidate of a new syndrome of cardiac and urogenital anomalies (CUGS) [27,32]. Shortly afterwards, further de novo variants in MYRF have been identified as the genetic cause of congenital diaphragmatic hernia (CDH) in patients that also presented congenital heart disease (CHD); three of the patients also had varying genital anomalies ranging from female external genitalia with a blind ending vagina to ambiguous genitalia and/or undescended testes, extending the spectrum of CUGS [4].

Additionally, variants in MYRF have been found in patients with eye conditions. For instance, Garnai and colleagues [6] identified a frameshift variant (c.769dupC, p.S264Qfs*74) in an eight year old male subject with nanophthalmos, an extreme form of hyperopia or farsightedness, who also presented cardiac and urogenital malformations, such as a mitral valve prolapse, a micropenis and unilateral cryptorchidism. In the same way, Xiao and colleagues [33] found a de novo frameshift variant (c.3274_3275del, p.L1093Pfs*22) in a six year old boy with high hyperopia and a splice-site variant (c.3194 + 2T>C) in a 40-year-old woman with high hyperopia that developed angle-closure glaucoma of both eyes. Familial cases of nanophthalmos due to disrupting variants of MYRF have also been identified. Garnai and colleagues also studied a large family with inherited nanophthalmos, and found a disrupting splice site variant (c.3376-1G>A, p.G1126Vfs*31), leading to a frameshift in the last exon. Four members of this family also had dextrocardia, and one of them also had a right hypoplastic lung and pulmonary artery stenosis. Shortly after, Xiao and colleagues [33], investigating another large family with inherited nanophthalmos, revealed an additional truncating mutation in MYRF (c.3377delG, p.G1126Vfs*31). Although the variants in the two large families identified by Garnai et al. [6] and Xiao et al. [33] were different, the effect on the protein was the same. Siggs and colleagues [34] also identified a large family with inherited autosomal nanophthalmos associated with a C-terminal frameshift

variant in *MYRF* (c.3361delC, p.R1121Gfs36*) introducing a premature terminal codon in the penultimate exon. These familial cases of nanophthalmos are mostly non-syndromic, leading to the speculation that the ocular tissue is more sensitive to haploinsufficiency than the cardiac and urogenital tissues [6]. On the other hand, little is known so far about the function of the C-terminal part of *MYRF* located in the ER membrane.

In addition to the association between *MYRF* variants with congenital heart defects and nanophthalmos, Hamanaka et al. described *MYRF* as a new candidate gene for DSD [7], after a case-control study comparing gene-based burdens of rare damaging variants between both groups. The authors described four new *MYRF* variants in five individuals from four families. From those, three patients were 46,XY and two were 46,XX. All of them presented different phenotypes of DSD; however, only one had a diaphragmatic hernia, and neither heart defects nor nanophthalmos were associated in those patients. More recently, Globa et al. [8] reported two other cases of *MYRF* heterozygous variants as a cause of DSD. Both individuals were 46,XY; the first one registered as a female with ambiguous genitalia, later raised as a boy, and the second one was a girl with primary amenorrhea, a lack of secondary sexual characteristics and high-grade hypermetropia. According to the authors, the *MYRF* loss-of-function variant described in this patient was the first case combining gonadal dysgenesis and nanophthalmos phenotypes. Here, we present the case of a 46,XY patient with PGD, Scimitar syndrome, pulmonary vein malformation and severe hyperopia, who, to the best of our knowledge, is the first case involving eye, heart and genital defects due to a *MYRF* disruptive variant.

Although the function of this gene in sex development pathways is still unclear, the association of heterozygous de novo variants with gonadal dysgenesis in both 46,XY and 46,XX individuals points to an important function in early gonadal development [4,7]. Based on our bioinformatics analyses utilizing scRNA-seq, we bring robust evidence that *MYRF* is expressed mainly in cells of the coelomic epithelium during early development of the bipotential gonads. Similar results were reported by Hamanaka et al. in 2019, using a different scRNA data set, thus corroborating our results. The coelomic epithelium constitutes the first layer of cells in the urogenital ridge at the fourth week post fertilization (wpf), and during the fifth wpf they proliferate, forming a thickened multi-layered cluster of cells that differentiates into the primordial gonad or gonadal ridge. Some of the CE cells transform into NR5A1-positive gonadal precursors that later differentiate into Sertoli and granulosa cells, as well as into steroidogenic cells [35]. At the same time, the primordial germ cells migrate from the hindgut into the NR5A1-positive gonadal precursor cells [36,37]. CE cells have an important role in the early development of the bipotential gonads. Therefore, disrupting variants in the *MYRF* gene, which is highly expressed in this cell population, could have an impact in the normal development of the gonads.

Of the differentially expressed genes with a binding site for *MYRF*, *CITED2* (OMIM * 602937) caught our special attention. *CITED2* is involved in early gonadal development and sex determination. In mice, *Cited2* is expressed in the urogenital ridge and cooperates with *Wt1* to stimulate the transcription of *Nr5a1* [29,38]. In addition, a physical interaction of *CITED2* and *WT1* was shown by immunoprecipitation (IP), as well as GST pulldown, revealing an interaction with both *WT1* isoforms (+/-KTS) [38]. Buaas et al. had shown that *CITED2* functions to ensure high expression levels from *Nr5a1* and *Sry*, providing a proper activation of the male pathway during sex development, and providing evidence that *Sry* is a downstream target of the *CITED2*/*WT1*/*NR5A1* regulatory pathway [29]. Moreover, reduced gene dosage of *Wt1* or *Nr5a1* in *Cited2* mutant gonads leads to partial sex reversal and can undergo complete XY sex reversal in the context of a hypomorphic *Sry* allele [29]. A transcriptional delay of male development in *Cited2*^{-/-} mice was reported by Combes et al. [30], due to a reduction of *Nr5a1* levels at early gonadal development. Furthermore, XX *Cited2*^{-/-} gonads showed defects in ovary differentiation with ectopic cell migration, transient upregulation of testis promoting factor *Fgf9* and delay of ovary promoting genes *Wnt4* and *Foxl2*, suggesting *Nr5a1* as an ovarian promoting gene. Human variants in *CITED2*, such as in *NR5A1*, are associated with premature ovarian

failure (POF) [39,40]. Our finding that, in humans, *CITED2* is found upregulated in *MYRF* positive cells of the coelomic epithelium of the ovaries and contains a *MYRF* binding site makes *MYRF* a potential candidate as a new upstream regulator of early gonadal development. Therefore, haploinsufficiency of this gene may lead to different forms of gonadal dysgenesis in 46,XX and 46,XY individuals, and *CITED2* might be an important downstream target of *MYRF*.

Interestingly, *CITED2* is also required for heart morphogenesis, as well as establishment of the left–right axis in humans and mice [31,41,42]. *Cited2*^{−/−} mice die during gestation with diverse cardiovascular malformations, such as atrial and ventricular septal defects (ASD/VSD), aberrant aortic arches, and common arterial trunk and left–right patterning defects [31,42], a phenotype very similar to that of patients with heterozygous de novo variants in *MYRF*. In humans, variants in *CITED2* were identified in patients with congenital heart defects (CHD) such as sinus venosus atrial septal defects, abnormal pulmonary venous return to the right atria, Tetralogy of Fallot, dextrocardia and other ventricular septal defects [41,43], also seen in patients with *MYRF* variants [44]. More importantly, several of these variants are localized in the promoter region of *CITED2* and have been proven to alter *CITED2* transcriptional activity, decreasing their expression [41,45]. Therefore, it is possible that haploinsufficiency of transcription factors of *CITED2*, such as *MYRF*, can influence its expression levels and lead to heart defects.

It is also important to highlight that according to an in silico prediction of the genome aggregation database (gnomAD v2.1.1) *MYRF* is a constraint gene and the value of pLI (probability of being loss-of-function intolerant) is 1, supported by a very low LOEUF (loss-of-function observed/expected upper bound fraction) value of 0.117, which means that this is a haploinsufficient gene, where loss of a single copy is not tolerated [46]. This is corroborated by the finding that, such as in our case, de novo variants are associated with most of the syndromic forms. In contrast, familiar cases of nanophthalmos are mostly associated with variants in the last exon, and other features of the CUGS are only seen in some individuals [6,33,34]. In the same way, no loss-of-function variants have been observed so far in *CITED2* in gnomAD, making *CITED2* a potential candidate of a downstream factor of *MYRF* whose reduced expression may induce the observed phenotypes in humans. Haploinsufficiency is frequently observed in cases of DSD produced by heterozygous variants or copy number variations in transcription factors such as *NR5A1*, *SOX9*, *NR0B1* or *WT1*, demonstrating that sex determination is highly sensitive to gene dosage [47–49]. Therefore, phenotypic variability of *MYRF* haploinsufficiency on gonadal development was expected since it acts in the same pathway. Nevertheless, further epigenetic and transcriptome studies in the respective gonadal and/or heart tissues will be necessary to elucidate the pleiotropic developmental effects of *MYRF* variants in the context of gene regulation and protein interaction.

5. Conclusions

Our data give evidence that heterozygous inactivating variants in *MYRF* may influence the upregulation of *CITED2* and thereby impact the *NR5A1* pathway of sex development very early in the gonadal ridge of both sexes, which might make *MYRF* haploinsufficiency a feasible cofactor disease due to missing upregulation of *CITED2*. Further investigations are needed to elucidate the interaction between *MYRF* and *CITED2*. In addition, a missing upregulation of *CITED2* by *MYRF* in heart development might also be the cause for abnormal pulmonary venous return to the right atria, atrial septal defect (ASD) or tetralogy of Fallot (ToF), as well as a left–right patterning defect that is observed in humans with heterozygous *CITED2* variants and *Cited2*^{−/−} mice [31,41]. Heterozygous variants in *MYRF* are also associated with nanophthalmos. To our knowledge, we present the first case with a combination of three *MYRF* associated phenotypic features: heart defects (CHD, dextrocardia, anomalous pulmonary venous return), 46,XY PGD and severe hyperopia. A reason for this might be the very recent description of the CUGS, as well as the separate detection of C-terminal *MYRF* variants in familiar cases of nanophthalmos without further

CUGS symptoms and the different time points of diagnosis. While cardiac failures are detected at birth, nanophthalmos might be only detected during the first years of childhood, and gonadal dysgenesis is often only detected at puberty, all by different specialists, making a common diagnosis often difficult.

Supplementary Materials: The following supporting information can be downloaded at: <https://www.mdpi.com/article/10.3390/jcm11164858/s1>, Figure S1: Heatmap of the mean expression value in each cell cluster of the marker genes used to identify the cell populations found in testes samples; Figure S2: Heatmap of the mean expression value in each cell cluster of the marker genes used to identify the cell populations found in ovaries samples; Figure S3: Violin plot showing *MYRF* gene expression values in each cell population. Each dot represents the normalized expression value of *MYRF* in a cell. Cell clusters with less than ten cells were discarded. Table S1: List of samples reanalysed in this study derived from previous publications and deposited in the Gene Expression Omnibus database (GEO).

Author Contributions: Conceptualization, R.W.; formal analysis, V.C.-S., A.K., H.B. and F.O.; investigation, R.W. and M.A.-S.; writing—original draft preparation, R.W., V.C.-S. and H.F.-S.; writing—review and editing, R.W., O.H., L.W. and H.B.; visualization, V.C.-S. and H.F.-S.; supervision, R.W. and H.B.; funding acquisition, O.H. and H.B. All authors have read and agreed to the published version of the manuscript.

Funding: This work was funded by financial support from Bundesministerium für Bildung und Forschung BMBF (01DQ17004) and Deutsche Forschungsgemeinschaft (DFG, German Research Foundation) under Germany's Excellence Strategy (EXC 22167- 390884018) and Bundesministerium für Gesundheit (BMG). V.C.-S. and O.H. have received funding by the German Ministry of Health (grant No. 2519FSB503) for the project "Standardized and centred care for DSD over the lifespan (DSDCare)". H.F.-S. received a scholarship from Fundação de Amparo à Pesquisa do Estado de São Paulo (FAPESP #2020/13421-8) and by the Alexander von Humboldt Fellowship. M.A.-S. received a DAAD scholarship within the German Egyptian Research Long-term Scholarship (GERLS) Programme, 2019, No. 57460069. The funders had no role in study design, data collection and analysis, decision to publish, or preparation of the manuscript.

Institutional Review Board Statement: The study was conducted according to the guidelines of the Declaration of Helsinki and approved by the local Ethics Committee of the University of Lübeck (AZ08-081, AZ17-219).

Informed Consent Statement: Written informed consent including pseudonymised publication of scientific results was obtained from the parents/legal guardians of the patient.

Data Availability Statement: The data presented in this study were previously published and are openly available in NCBI's Gene Expression Omnibus [50], and are accessible through GEO Series accession number GSE143380 [20], GSE143356 [20], GSE124263 [17], GSE161617 [19] and GSE134144 [18].

Acknowledgments: V.C.-S., F.O., A.K. and H.B. acknowledge computational support from the OMICS compute cluster at the University of Lübeck.

Conflicts of Interest: The authors declare no conflict of interest.

References

1. Emery, B.; Agalliu, D.; Cahoy, J.D.; Watkins, T.A.; Dugas, J.C.; Mulinyawe, S.B.; Ibrahim, A.; Ligon, K.L.; Rowitch, D.H.; Barres, B.A. Myelin gene regulatory factor is a critical transcriptional regulator required for CNS myelination. *Cell* **2009**, *138*, 172–185. [[CrossRef](#)] [[PubMed](#)]
2. Koening, M.; Jackson, S.; Hay, C.M.; Faux, C.; Kilpatrick, T.J.; Willingham, M.; Emery, B. Myelin gene regulatory factor is required for maintenance of myelin and mature oligodendrocyte identity in the adult CNS. *J. Neurosci. Off. J. Soc. Neurosci.* **2012**, *32*, 12528–12542. [[CrossRef](#)] [[PubMed](#)]
3. Bujalka, H.; Koening, M.; Jackson, S.; Perreau, V.M.; Pope, B.; Hay, C.M.; Mitew, S.; Hill, A.F.; Lu, Q.R.; Wegner, M.; et al. MYRF is a membrane-associated transcription factor that autoproteolytically cleaves to directly activate myelin genes. *PLoS Biol.* **2013**, *11*, e1001625. [[CrossRef](#)] [[PubMed](#)]

4. Qi, H.; Yu, L.; Zhou, X.; Wynn, J.; Zhao, H.; Guo, Y.; Zhu, N.; Kitaygorodsky, A.; Hernan, R.; Aspelund, G.; et al. De novo variants in congenital diaphragmatic hernia identify MYRF as a new syndrome and reveal genetic overlaps with other developmental disorders. *PLoS Genet.* **2018**, *14*, e1007822. [[CrossRef](#)] [[PubMed](#)]
5. Jin, S.C.; Homsy, J.; Zaidi, S.; Lu, Q.; Morton, S.; DePalma, S.R.; Zeng, X.; Qi, H.; Chang, W.; Sierant, M.C.; et al. Contribution of rare inherited and de novo variants in 2871 congenital heart disease probands. *Nat. Genet.* **2017**, *49*, 1593–1601. [[CrossRef](#)] [[PubMed](#)]
6. Garnai, S.J.; Brinkmeier, M.L.; Emery, B.; Aleman, T.S.; Pyle, L.C.; Veleva-Rotse, B.; Sisk, R.A.; Rozsa, F.W.; Ozel, A.B.; Li, J.Z.; et al. Variants in myelin regulatory factor (MYRF) cause autosomal dominant and syndromic nanophthalmos in humans and retinal degeneration in mice. *PLoS Genet.* **2019**, *15*, e1008130. [[CrossRef](#)]
7. Hamanaka, K.; Takata, A.; Uchiyama, Y.; Miyatake, S.; Miyake, N.; Mitsuhashi, S.; Iwama, K.; Fujita, A.; Imagawa, E.; Alkanaq, A.N.; et al. MYRF haploinsufficiency causes 46,XY and 46,XX disorders of sex development: Bioinformatics consideration. *Hum. Mol. Genet.* **2019**, *28*, 2319–2329. [[CrossRef](#)]
8. Globa, E.; Zelinska, N.; Shcherbak, Y.; Bignon-Topalovic, J.; Bashamboo, A.; Msmall es, C.K. Disorders of Sex Development in a Large Ukrainian Cohort: Clinical Diversity and Genetic Findings. *Front. Endocrinol.* **2022**, *13*, 810782. [[CrossRef](#)]
9. Hughes, I.A.; Houk, C.; Ahmed, S.F.; Lee, P.A. Consensus statement on management of intersex disorders. *Arch. Dis. Child.* **2006**, *91*, 554–563. [[CrossRef](#)]
10. Capel, B. Vertebrate sex determination: Evolutionary plasticity of a fundamental switch. *Nat. Rev. Genet.* **2017**, *18*, 675–689. [[CrossRef](#)]
11. Elzaiai, M.; McElreavey, K.; Bashamboo, A. Genetics of 46,XY gonadal dysgenesis. *Best Pract. Res. Clin. Endocrinol. Metab.* **2022**, *36*, 101633. [[CrossRef](#)] [[PubMed](#)]
12. Stöhr, H.; Marquardt, A.; White, K.; Weber, B.H. cDNA cloning and genomic structure of a novel gene (C11orf9) localized to chromosome 11q12→q13.1 which encodes a highly conserved, potential membrane-associated protein. *Cytogenet Cell Genet* **2000**, *88*, 211–216. [[CrossRef](#)] [[PubMed](#)]
13. An, H.; Fan, C.; Sharif, M.; Kim, D.; Poitelon, Y.; Park, Y. Functional mechanism and pathogenic potential of MYRF ICA domain mutations implicated in birth defects. *Sci. Rep.* **2020**, *10*, 814. [[CrossRef](#)] [[PubMed](#)]
14. Li, H.; Durbin, R. Fast and accurate short read alignment with Burrows-Wheeler transform. *Bioinformatics* **2009**, *25*, 1754–1760. [[CrossRef](#)] [[PubMed](#)]
15. DePristo, M.A.; Banks, E.; Poplin, R.; Garimella, K.V.; Maguire, J.R.; Hartl, C.; Philippakis, A.A.; del Angel, G.; Rivas, M.A.; Hanna, M.; et al. A framework for variation discovery and genotyping using next-generation DNA sequencing data. *Nat. Genet.* **2011**, *43*, 491–498. [[CrossRef](#)]
16. Rausch, T.; Zichner, T.; Schlattl, A.; Stutz, A.M.; Benes, V.; Korbel, J.O. DELLY: Structural variant discovery by integrated paired-end and split-read analysis. *Bioinformatics* **2012**, *28*, i333–i339. [[CrossRef](#)] [[PubMed](#)]
17. Sohni, A.; Tan, K.; Song, H.W.; Burow, D.; de Rooij, D.G.; Laurent, L.; Hsieh, T.C.; Rabah, R.; Hammoud, S.S.; Vicini, E.; et al. The Neonatal and Adult Human Testis Defined at the Single-Cell Level. *Cell Rep.* **2019**, *26*, 1501–1517.e1504. [[CrossRef](#)]
18. Guo, J.; Nie, X.; Giebler, M.; Mlcochova, H.; Wang, Y.; Grow, E.J.; DonorConnect; Kim, R.; Tharmalingam, M.; Matilionyte, G.; et al. The Dynamic Transcriptional Cell Atlas of Testis Development during Human Puberty. *Cell Stem Cell* **2020**, *26*, 262–276.e264. [[CrossRef](#)]
19. Guo, J.; Sosa, E.; Chitiashvili, T.; Nie, X.; Rojas, E.J.; Oliver, E.; DonorConnect; Plath, K.; Hotaling, J.M.; Stukenborg, J.B.; et al. Single-cell analysis of the developing human testis reveals somatic niche cell specification and fetal germline stem cell establishment. *Cell Stem Cell* **2021**, *28*, 764–778.e764. [[CrossRef](#)]
20. Chitiashvili, T.; Dror, I.; Kim, R.; Hsu, F.M.; Chaudhari, R.; Pandolfi, E.; Chen, D.; Liebscher, S.; Schenke-Layland, K.; Plath, K.; et al. Female human primordial germ cells display X-chromosome dosage compensation despite the absence of X-inactivation. *Nat. Cell Biol.* **2020**, *22*, 1436–1446. [[CrossRef](#)]
21. Chen, S.; Zhou, Y.; Chen, Y.; Gu, J. fastp: An ultra-fast all-in-one FASTQ preprocessor. *Bioinformatics* **2018**, *34*, i884–i890. [[CrossRef](#)] [[PubMed](#)]
22. Melsted, P.; Boeshaghi, A.S.; Liu, L.; Gao, F.; Lu, L.; Min, K.H.J.; da Veiga Beltrame, E.; Hjørleifsson, K.E.; Gehring, J.; Pachter, L. Modular, efficient and constant-memory single-cell RNA-seq preprocessing. *Nat. Biotechnol.* **2021**, *39*, 813–818. [[CrossRef](#)] [[PubMed](#)]
23. Hao, Y.; Hao, S.; Andersen-Nissen, E.; Mauck, W.M., 3rd; Zheng, S.; Butler, A.; Lee, M.J.; Wilk, A.J.; Darby, C.; Zager, M.; et al. Integrated analysis of multimodal single-cell data. *Cell* **2021**, *184*, 3573–3587.e3529. [[CrossRef](#)] [[PubMed](#)]
24. Roselli, S.; Gribouval, O.; Boute, N.; Sich, M.; Benessy, F.; Attie, T.; Gubler, M.C.; Antignac, C. Podocin localizes in the kidney to the slit diaphragm area. *Am. J. Pathol.* **2002**, *160*, 131–139. [[CrossRef](#)]
25. Rudat, C.; Grieskamp, T.; Rohr, C.; Airik, R.; Wrede, C.; Hegermann, J.; Herrmann, B.G.; Schuster-Gossler, K.; Kispert, A. Upk3b is dispensable for development and integrity of urothelium and mesothelium. *PLoS ONE* **2014**, *9*, e112112. [[CrossRef](#)] [[PubMed](#)]
26. Richards, S.; Aziz, N.; Bale, S.; Bick, D.; Das, S.; Gastier-Foster, J.; Grody, W.W.; Hegde, M.; Lyon, E.; Spector, E.; et al. Standards and guidelines for the interpretation of sequence variants: A joint consensus recommendation of the American College of Medical Genetics and Genomics and the Association for Molecular Pathology. *Genet. Med. Off. J. Am. Coll. Med. Genet.* **2015**, *17*, 405–424. [[CrossRef](#)]

27. Pinz, H.; Pyle, L.C.; Li, D.; Izumi, K.; Skraban, C.; Tarpinian, J.; Braddock, S.R.; Telegrafi, A.; Monaghan, K.G.; Zackai, E.; et al. De novo variants in Myelin regulatory factor (MYRF) as candidates of a new syndrome of cardiac and urogenital anomalies. *Am. J. Med. Genet. Part A* **2018**, *176*, 969–972. [[CrossRef](#)]
28. Fishilevich, S.; Nudel, R.; Rappaport, N.; Hadar, R.; Plaschkes, I.; Iny Stein, T.; Rosen, N.; Kohn, A.; Twik, M.; Safran, M.; et al. GeneHancer: Genome-wide integration of enhancers and target genes in GeneCards. *Database* **2017**, *2017*, bax028. [[CrossRef](#)]
29. Buaas, F.W.; Val, P.; Swain, A. The transcription co-factor CITED2 functions during sex determination and early gonad development. *Hum. Mol. Genet.* **2009**, *18*, 2989–3001. [[CrossRef](#)]
30. Combes, A.N.; Spiller, C.M.; Harley, V.R.; Sinclair, A.H.; Dunwoodie, S.L.; Wilhelm, D.; Koopman, P. Gonadal defects in Cited2-mutant mice indicate a role for SF1 in both testis and ovary differentiation. *Int. J. Dev. Biol.* **2010**, *54*, 683–689. [[CrossRef](#)]
31. Weninger, W.J.; Lopes Floro, K.; Bennett, M.B.; Withington, S.L.; Preis, J.I.; Barbera, J.P.; Mohun, T.J.; Dunwoodie, S.L. Cited2 is required both for heart morphogenesis and establishment of the left-right axis in mouse development. *Development* **2005**, *132*, 1337–1348. [[CrossRef](#)] [[PubMed](#)]
32. Chitayat, D.; Shannon, P.; Uster, T.; Nezarati, M.M.; Schnur, R.E.; Bhoj, E.J. An Additional Individual with a De Novo Variant in Myelin Regulatory Factor (MYRF) with Cardiac and Urogenital Anomalies: Further Proof of Causality: Comments on the article by Pinz et al. *Am. J. Med. Genet. Part A* **2018**, *176*, 2041–2043. [[CrossRef](#)] [[PubMed](#)]
33. Xiao, X.; Sun, W.; Ouyang, J.; Li, S.; Jia, X.; Tan, Z.; Hejtmancik, J.F.; Zhang, Q. Novel truncation mutations in MYRF cause autosomal dominant high hyperopia mapped to 11p12-q13.3. *Hum. Genet.* **2019**, *138*, 1077–1090. [[CrossRef](#)] [[PubMed](#)]
34. Siggs, O.M.; Souzeau, E.; Breen, J.; Qassim, A.; Zhou, T.; Dubowsky, A.; Ruddie, J.B.; Craig, J.E. Autosomal dominant nanophthalmos and high hyperopia associated with a C-terminal frameshift variant in MYRF. *Mol. Vis.* **2019**, *25*, 527–534.
35. Stevant, I.; Kuhne, F.; Greenfield, A.; Chaboissier, M.C.; Dermitzakis, E.T.; Nef, S. Dissecting Cell Lineage Specification and Sex Fate Determination in Gonadal Somatic Cells Using Single-Cell Transcriptomics. *Cell Rep.* **2019**, *26*, 3272–3283.e3273. [[CrossRef](#)] [[PubMed](#)]
36. Piprek, R.P.; Kloc, M.; Kubiak, J.Z. Early Development of the Gonads: Origin and Differentiation of the Somatic Cells of the Genital Ridges. *Results Probl. Cell Differ.* **2016**, *58*, 1–22. [[CrossRef](#)] [[PubMed](#)]
37. Pelosi, E.; Koopman, P. Development of the Testis. In *Reference Module in Biomedical Sciences*; Elsevier: Amsterdam, The Netherlands, 2017; pp. 1–8.
38. Val, P.; Martinez-Barbera, J.P.; Swain, A. Adrenal development is initiated by Cited2 and Wt1 through modulation of Sf-1 dosage. *Development* **2007**, *134*, 2349–2358. [[CrossRef](#)]
39. Lourenco, D.; Brauner, R.; Lin, L.; De Perdigo, A.; Weryha, G.; Muresan, M.; Boudjenah, R.; Guerra-Junior, G.; Maciel-Guerra, A.T.; Achermann, J.C.; et al. Mutations in NR5A1 associated with ovarian insufficiency. *N. Engl. J. Med.* **2009**, *360*, 1200–1210. [[CrossRef](#)]
40. Fonseca, D.J.; Ojeda, D.; Lakhal, B.; Braham, R.; Eggers, S.; Turbitt, E.; White, S.; Grover, S.; Warne, G.; Zacharin, M.; et al. CITED2 mutations potentially cause idiopathic premature ovarian failure. *Transl. Res.* **2012**, *160*, 384–388. [[CrossRef](#)]
41. Sperling, S.; Grimm, C.H.; Dunkel, I.; Mebus, S.; Sperling, H.P.; Ebner, A.; Galli, R.; Lehrach, H.; Fusch, C.; Berger, F.; et al. Identification and functional analysis of CITED2 mutations in patients with congenital heart defects. *Hum. Mutat.* **2005**, *26*, 575–582. [[CrossRef](#)]
42. Bamforth, S.D.; Braganca, J.; Farthing, C.R.; Schneider, J.E.; Broadbent, C.; Michell, A.C.; Clarke, K.; Neubauer, S.; Norris, D.; Brown, N.A.; et al. Cited2 controls left-right patterning and heart development through a Nodal-Pitx2c pathway. *Nat. Genet.* **2004**, *36*, 1189–1196. [[CrossRef](#)] [[PubMed](#)]
43. Yang, X.F.; Wu, X.Y.; Li, M.; Li, Y.G.; Dai, J.T.; Bai, Y.H.; Tian, J. Mutation analysis of Cited2 in patients with congenital heart disease. *Zhonghua Er Ke Za Zhi* **2010**, *48*, 293–296. [[PubMed](#)]
44. Rossetti, L.Z.; Glington, K.; Yuan, B.; Liu, P.; Pillai, N.; Mizerik, E.; Magoulas, P.; Rosenfeld, J.A.; Karaviti, L.; Sutton, V.R.; et al. Review of the phenotypic spectrum associated with haploinsufficiency of MYRF. *Am. J. Med. Genet. Part A* **2019**, *179*, 1376–1382. [[CrossRef](#)] [[PubMed](#)]
45. Zheng, S.Q.; Chen, H.X.; Liu, X.C.; Yang, Q.; He, G.W. Genetic analysis of the CITED2 gene promoter in isolated and sporadic congenital ventricular septal defects. *J. Cell Mol. Med.* **2021**, *25*, 2254–2261. [[CrossRef](#)] [[PubMed](#)]
46. Lek, M.; Karczewski, K.J.; Minikel, E.V.; Samocha, K.E.; Banks, E.; Fennell, T.; O'Donnell-Luria, A.H.; Ware, J.S.; Hill, A.J.; Cummings, B.B.; et al. Analysis of protein-coding genetic variation in 60,706 humans. *Nature* **2016**, *536*, 285–291. [[CrossRef](#)]
47. Werner, R.; Mönig, I.; August, J.; Freiberg, C.; Lünstedt, R.; Reiz, B.; Wünsch, L.; Holterhus, P.M.; Kulle, A.; Döhnert, U.; et al. Novel Insights into 46,XY Disorders of Sex Development due to NR5A1 Gene Mutation. *Sex. Dev. Genet. Mol. Biol. Evol. Endocrinol. Embryol. Pathol. Sex Determ. Differ.* **2015**, *9*, 260–280. [[CrossRef](#)]
48. Croft, B.; Ohnesorg, T.; Hewitt, J.; Bowles, J.; Quinn, A.; Tan, J.; Corbin, V.; Pelosi, E.; van den Bergen, J.; Sreenivasan, R.; et al. Human sex reversal is caused by duplication or deletion of core enhancers upstream of SOX9. *Nat. Commun.* **2018**, *9*, 5319. [[CrossRef](#)]
49. Eozenou, C.; Gonen, N.; Touzon, M.S.; Jorgensen, A.; Yatsenko, S.A.; Fusee, L.; Kamel, A.K.; Gellen, B.; Guercio, G.; Singh, P.; et al. Testis formation in XX individuals resulting from novel pathogenic variants in Wilms' tumor 1 (WT1) gene. *Proc. Natl. Acad. Sci. USA* **2020**, *117*, 13680–13688. [[CrossRef](#)]
50. Edgar, R.; Domrachev, M.; Lash, A.E. Gene Expression Omnibus: NCBI gene expression and hybridization array data repository. *Nucleic Acids Res.* **2002**, *30*, 207–210. [[CrossRef](#)]